

Improved photocatalytic performances for La-doped one-dimensional ZnO/MXene composites

B. Zeng^{a,*}, X. T. Ning^b, L. F. Li^a, R. X. Wang^a

^a*College of Mechanical Engineering, Hunan University of Arts and Science, Changde 415000, People's Republic of China*

^b*School of Materials and Environmental Engineering, Hunan University of Humanities, Science, 415000, Loudi 417000, People's Republic of China*

La-doped one-dimensional ZnO/MXene composites (La-1D-ZnO/MXene) were prepared by applying a microwave-assisted aqueous solution method. The extracted experimental results showed that ZnO nanoparticles had an olive-like morphology and MXene had a layer structure with nanoparticles uniformly distributed on their surface. The products were systematically characterized by using scanning electronic microscopy (SEM), transmission electron microscopy (TEM), X-ray diffraction (XRD), UV-vis absorption spectroscopy, photoluminescence spectroscopy (PL) and X-ray photoelectron spectroscopy (XPS). The photocatalytic degradation test indicated that the La-1D-ZnO/MXene showed good photocatalytic performance and about 94.8% methyl orange (MO) was degraded within 120 min. This behavior could be attributed to the synergistic effects of the increased active sites, enhanced visible light absorption, and accelerated charge transferring. Therefore, the proposed synthesized nanohybrids could be regarded as a promising candidate for the future development of novel catalytic devices.

(Received April 16, 2022; Accepted August 11, 2022)

Keywords: MXene, Doped, Photocatalytic

1. Introduction

The semiconductor-based photocatalysis technology is considered one of the most effective approaches for alleviating environmental pollution^[1]. Along these lines, due to their photo-stability and nontoxicity, ZnO is regarded as a promising material in the application of photocatalysis^[2]. With its large surface area and good resistance to photocorrosion, one-dimensional (1D) ZnO can provide abundant active sites^[3]. For that reason, is regarded as an excellent potential candidate for photocatalyst. However, its fast carrier recombination rate and wide band gap result in low photocatalytic efficiency and poor visible light absorption^[4].

Owing to its two-dimensional structure and excellent conductive properties, MXene can serve as an ideal conducting matrix and promote the separation of photoexcited charges, which is widely used in the fields of photocatalytic degradation^[5, 6]. Especially, the fabrication of MXene/semiconductor Schottky junction can prevent the photo-generated electrons from recombining and thus prolong the carrier lifetime^[7].

Additionally, lanthanide ions doped with ZnO can significantly enhance photocatalytic efficiency by the virtue of the following two factors^[8, 9]. Firstly, doping with lanthanide ions could lead to the formation of intraband gap states, which are below the CB of ZnO, thus significantly narrowing the wide band gap and resulting in efficient light utilization. Secondly, lanthanide ions can act as efficient scavengers to trap photogenerated electrons, preventing hence the recombination of the photo-excited charge carriers. In this context, the development of a novel photocatalyst with enriched active sites, enhanced visible light absorption, and accelerated charge transferring has attracted considerable attention from the scientific community.

Under this direction, in this work, La-doped ZnO/MXene photocatalysts with olive-like

* Corresponding author: 21467855@qq.com
<https://doi.org/10.15251/DJNB.2022.173.881>

ZnO anchoring on MXene nanosheets have been successfully fabricated. The unique one-dimensional/two-dimensional hybrid configuration with a doped band structure showed improved photocatalytic performance with 94.8% degradation of MO in 120 min under the impact of the simulated solar light irradiation. Finally, the mechanism for the improved photocatalytic performance was thoroughly investigated.

2. Experimental details

2.1. Materials and reagents

MXene was purchased from Deyang Carbonene technology Co. Ltd. All other reagents were supplied by Aladdin Industrial Corp.

2.2 Synthesis of samples

To prepare the La-1D-ZnO/MXene configuration, 90 ml of $Zn(AC)_2$, 10 ml of $La(NO_3)_3$, 9 g of MXene (0.5 wt.%) and 10 g of NaOH (8 wt.%) were continuously stirred for 30 minutes and then reacted for 30 min within a microwave chemical reactor (MCR-3). The reacted products were washed with DI water and the obtained solid was heated at 500 °C for 2 hours. 1D-ZnO/MXene sample was prepared under the same conditions without adding $La(NO_3)_3$. Besides, the 1D-ZnO sample was prepared with similar conditions without the addition of $La(NO_3)_3$ and MXene. ZnO NP, and ZnO NP/MXene were also fabricated according to the literature [2].

2.3. Characterization

The surface morphology of our prototypes was investigated by conducting scanning electron microscopy (SEM, Hitachi S4800) and transmission electron microscopy (TEM, JEOL JEM-2100F) measurements. X-ray diffraction (XRD, Bruker D2 PHASER) was also performed to characterize the phase of the composites. UV-Vis spectroscopy (UV-2550, Shimadzu) was also used to determine the absorbance spectrum and a spectrometer (IHR550, Horiba) was used to collect the photoluminescence spectra. X-ray photoelectron spectroscopy (XPS, Thermo K-Alpha) measurements were carried out to determine the chemical composition and the binding states of the composites.

2.4. Photocatalytic Experiment

The photocatalytic properties of our samples were tested through the removal reaction of methyl orange (MO). More specifically, 300 mg of the photocatalyst was dispersed into 300 mL MO with a rate as high as 10 mg L⁻¹, and the mixed solution was then stirred in the dark for 30 min. Subsequently, the solution was irradiated by solar light irradiation and 2.5 mL of reaction samples were collected at regular intervals of 20 min, centrifuged to remove any suspended solids. The concentrations of the MO dyes in an aqueous solution were monitored by using UV-vis spectroscopy based on the characteristic absorption peak centered at 464 nm. The removal efficiency was calculated according to the following equation $\eta = (1 - C/C_0) \times 100\%$, where η is the photodegradation (%), C and C₀ stand for the concentrations of MO after and before the visible-light irradiation, respectively.

3. Results and discussion

The structure of the La-1D-ZnO/MXene configuration was investigated by studying the X-ray diffraction (XRD) patterns, as is shown in Fig. 1. The recorded peaks at 31.8°, 34.5°, 36.4°, 47.8°, 56.7°, 62.5°, and 67.8° could be attributed to the existence of the (100), (002), (101), (102), (110), (103), and (112) planes of the hexagonal wurtzite ZnO (JCPDS 65-3411)^[10]. On top of that, the peaks at 19.3°, 27.8° represented the (004) and (006) planes of MXene^[11]. These results proved the successful formation of the ZnO and MXene composites.

As far as the photoluminescence (PL) spectra are concerned, they represented the

recombination rate of the photo-generated electrons-holes in the materials. As is shown in Fig. 2, under the excitation of 370 nm, the acquired PL spectrum of the 1D-ZnO structure revealed the existence of a high-intensity peak at 415 nm and 460 nm. In contrast, the PL intensity of the La-1D-ZnO/MXene structure was very weak. The recorded decrease in the PL intensity could be associated with the efficient charge separation^[12], thus improving the photocatalytic activity of the ZnO.

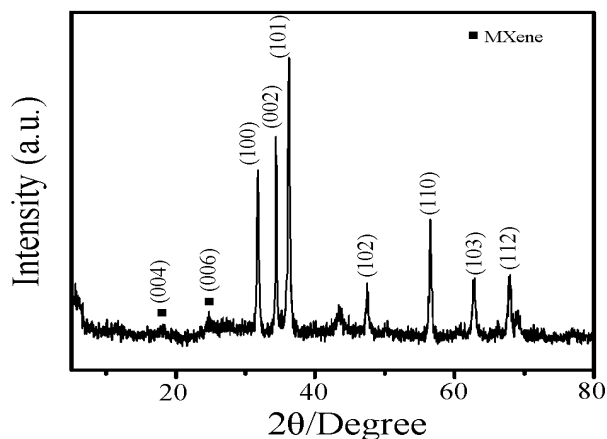


Fig. 1. (a) X-ray diffraction of La-1D-ZnO/MXene.

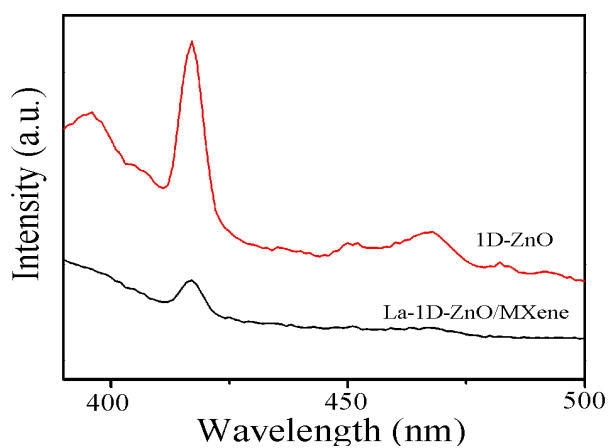


Fig. 2. Room temperature PL spectra of the samples.

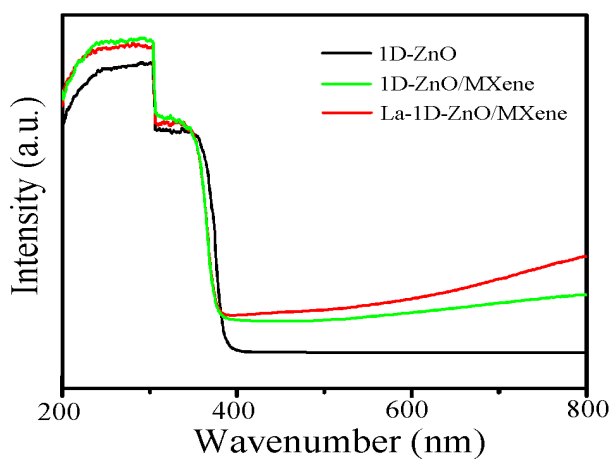


Fig. 3. UV-Vis diffuse reflectance absorption spectra of the samples.

The UV-Vis diffuse reflectance absorption spectra of the samples are shown in Fig. 3. For the pure 1D-ZnO configuration, the absorption peak at 200-380 nm could be clearly seen. As far as the ZnO/MXene structure is concerned, it extended the optical absorption into the visible light region, proving hence that MXene had a good light reaction^[13]. Through the La doping modification, the visible light absorption in the La-1D-ZnO/MXene was further improved due to the narrowed band gap of the ZnO^[14]. Therefore, it could be concluded that both MXene and La-doped facilitate the usage of the light utilization and thus induce a photocatalytic performance enhancement.

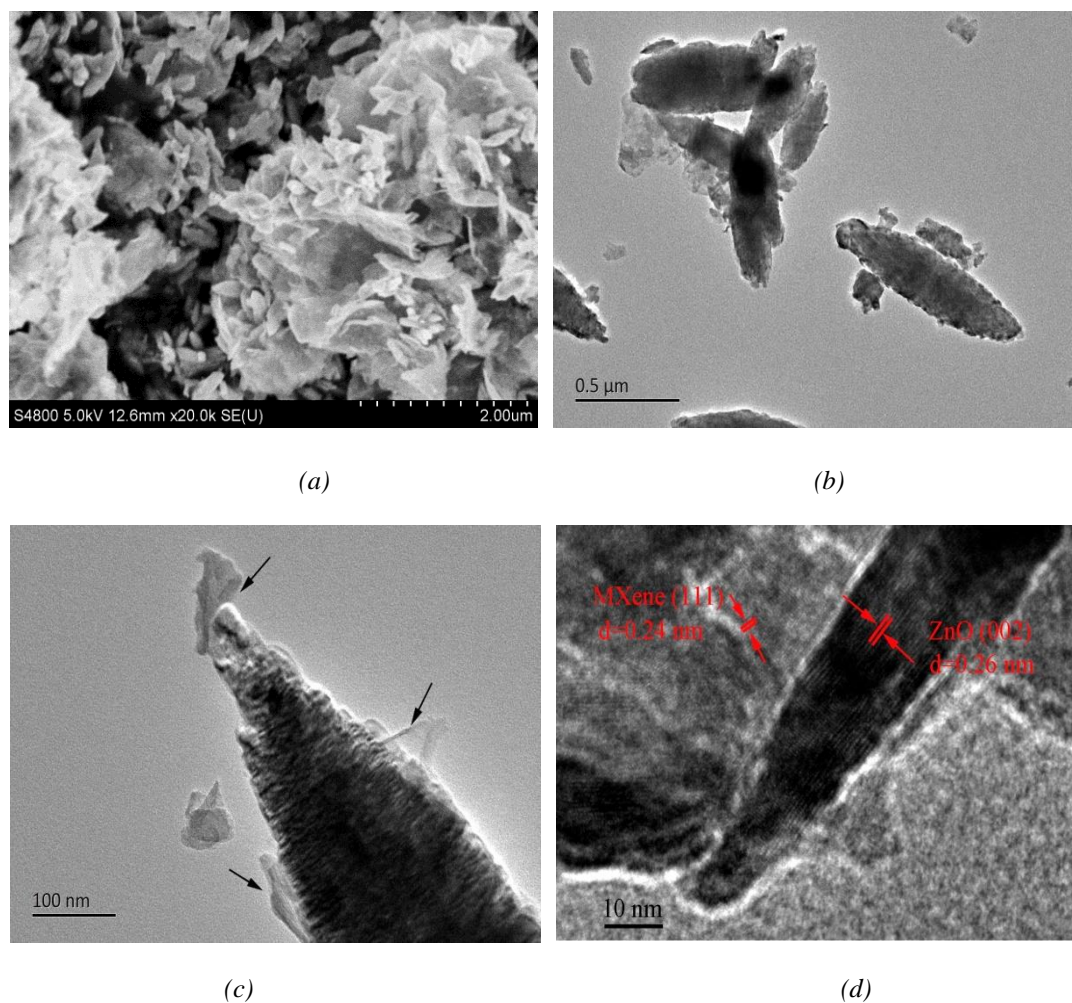


Fig. 4. (a) (b)SEM, (c) SEM, (d)HRTEM of La-1D-ZnO/MXene.

The morphology of the La-1D-ZnO/MXene material is shown in Fig. 4. The acquired SEM image (Fig. 4a) reveals that MXene possessed wrinkles and clear edges with olive-like nanoparticles that were distributed uniformly on their surface. From the TEM image depicted in Fig. 4b, olive-shaped nanoparticles were wrapped by MXene sheets with 300 nm diameter and a length in the range of 1-2 μ m. The enlarged TEM image further confirmed the intimate contact between ZnO nanoparticles and MXene (as is shown in Fig. 4c by the arrows). The HRTEM in Fig. 4d presents the existence of two lattice fringes with a lattice spacing of 0.24 nm corresponding to the (111) crystal plane of MXene and 0.26 nm corresponding to the (002) crystal plane of ZnO^[15].

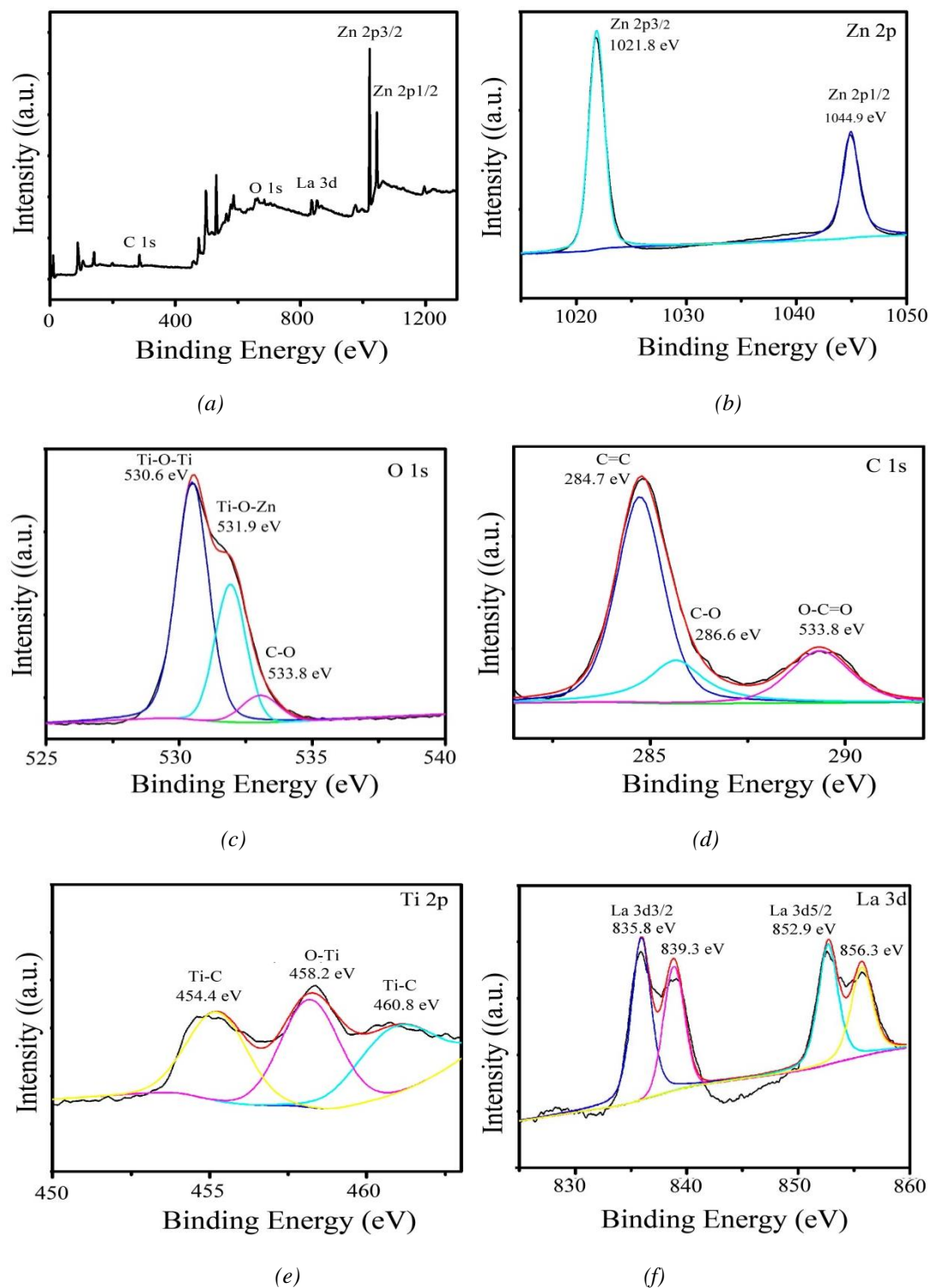


Fig. 5. Typical XPS spectra of the La-1D-ZnO/MXene composite: (a) survey spectra, (b) Zn 2p region XPS spectrum, (c) O 2p region XPS spectrum, (d) C 1s region XPS spectrum, (e) Ti 2p region XPS spectrum, (f) La 3d region XPS spectrum.

The surface chemical composition of the products was investigated by carrying out XPS analysis and the fully scanned XPS spectrum (Fig. 5a) of the La-1D-ZnO/MXene composite showed the existence of the following elements: Zn, O, Ti, C, and La. Moreover, two peaks at 1021.8 eV and 1044.9 eV are depicted in Fig. 5b, which correspond to the binding energies of Zn 2p_{1/2} and Zn 2p_{3/2}, confirming thus the presence of Zn²⁺ in the composite^[13]. In the O 1s

spectrum (Fig. 5c), the recorded peaks at 530.6 eV could be ascribed to the formation of the Zn-O-Zn bonds, which proved the formation of wurtzite ZnO. The peaks located at 531.9 eV and 533.8 eV could be originated from the formation of the Ti-O-Zn and C-O bond in the composites, indicating the manifestation of a strong interaction between ZnO and MXene^[13]. From the deconvolution process of the C1s region (Fig. 5d), three resolved peaks at 284.8 eV, 286.6 eV, and 289.4 eV were detected that are related to the C=C, C-O, and O-C=O bonds, respectively^[13]. In the high-resolution Ti 2p XPS spectrum (Fig. 5e), the peaks at 454.4 eV and 460.8 eV corresponded to the Ti-C bond. The band energy at 458.2eV was due to the formation of the O-Ti bond. This outcome proved the formation of Schottky junctions between ZnO and MXene. In Fig. 5f, the main peaks recorded at 835.8 and 852.9 eV could be assigned to La 3d5/2 and La 3d3/2, respectively, while the peaks at 839.3 and 856.3 eV represent the shake-up satellite peaks of La 3d5/2 and La 3d3/2. This result indicates the successful doping of La³⁺ into the ZnO lattice^[16].

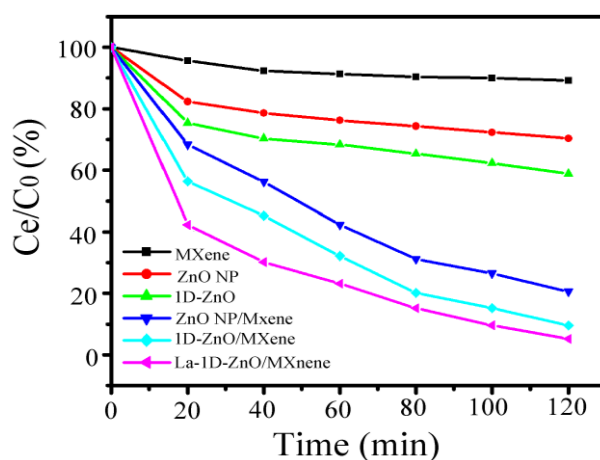


Fig. 6. Photocatalytic degradation efficiency of MO with different catalysts under visible light.

The photodegradation efficiency of MO in the simulated solar light was tested in the following material configurations: MXene, ZnO NP, 1D-ZnO, ZnO NP/MXene, 1D-ZnO/MXene and La-1D-ZnO/MXene. More specifically, the photodegradation efficiency of MO by MXene was 10.8%, which was almost negligible. As far as ZnO NP and 1D-ZnO are concerned, the photodegradation efficiency was increased to 29.7% and 41.2%, showing an obvious increase under solar light stimulation. In the case of ZnO NP/MXene, a degradation of about 79.4% was achieved, indicating that MXene could be served as a cocatalyst to improve the photocatalytic effect of ZnO. For the 1D-ZnO/MXene structure, the degraded efficiency of MO was increased up to the value of 90.4% and the underlying reason for this effect was that the one-dimensional morphology could possess outstanding performance due to the existence of abundant active sites and the manifestation of excellent electrical properties. With the La doping, the La-1D-ZnO/MXene structure could also obtain a 94.8% efficiency for the degradation of MO. The highest photocatalytic efficiency in all samples was ascribed to the one-dimensional structure ZnO, the conducting Mexene matrix and the lanthanide doping.

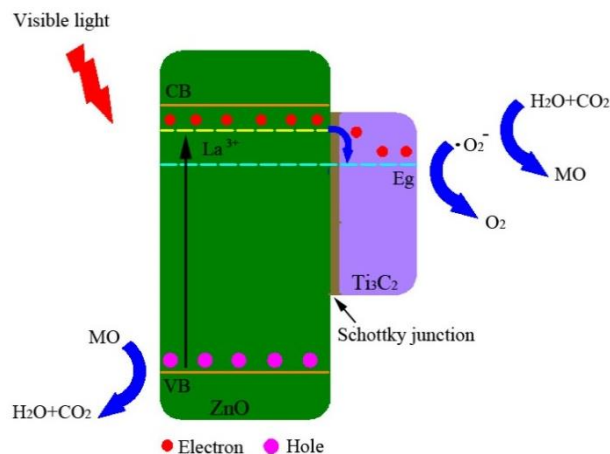


Fig. 7. Schematic photocatalytic reaction mechanism for La-1D-ZnO/MXene composite.

The prevailing photocatalytic mechanism is shown in Fig. 7. Under the solar light irradiation stimulation, only a small amount of electrons could be excited from the VB to the CB in ZnO due to their wide band gap^[17]. La doping could also induce the formation of intraband gap states and narrow the band gap of ZnO, which remarkably extended the adsorption of catalyst to the visible light region^[18]. Therefore, under solar light irradiation, photo-electron could be generated in the La-ZnO. Since the energy band location of the photo-generated electron was more negative than the Fermi level of MXene, excited electrons could be transferred to the MXene structure. At the same time, the formed Schottky junction between ZnO and MXene could effectively hinder the photogenerated electrons from returning to ZnO, thus preventing the recombination of the photo-generated electrons and holes^[19]. The excited electrons reacted also with O₂, forming thus super oxide anion radicals ($\bullet\text{O}_2^-$). Both super oxide anion radicals and holes left in the CB could decompose MO into CO₂ and H₂O^[20].

4. Conclusions

In summary, the La-1D-ZnO/MXene was successfully fabricated by using a microwave-assisted aqueous solution method and their degradation rate to MO reached the value of 94.8%. The one-dimensional structure is assumed to offer more active sites, whereas MXene effectively boosted the transfer of the photo-induced electrons. Additionally, the narrowed band gap of the ZnO was improved by La-doping and visible light absorption, which provided a synergistic effect in the enhancement of the photocatalytic performance. The proposed synthetic strategy could be extended to fabricate a series of novel MXene-based photocatalysts for environment-related applications.

Acknowledgments

This work was supported by the Science and Technology Bureau projects of Changde ([2019]21), Hunan Provincial Specialty Disciplines of Higher Education Institutions (XJT[2018]469), the Excellent Youth Program of Hunan Education Department (Grant No. 20B401), Key project of Hunan Provincial Education Department (18A361), Innovative Research Team in Higher Educational Institutions of Hunan Province XJT[2019]379).

References

- [1] F Wang, Q Li, D. Xu. *J. Mater. Chem. A* 8, 14863 (2020);
<https://doi.org/10.1039/D0TA04977H>
- [2] F.M.Sanakousar, C.C.Vidyasagar, V.M.Jiménez-Pérez, et al., *Materi. Sci. Semicon. Proc.* 140, 106390 (2022); <https://doi.org/10.1016/j.mssp.2021.106390>
- [3] X.B. Dong, P. Yang, Y. S. Liu et al., *Ceram. Int.* 42, 518 (2016);
<https://doi.org/10.1016/j.ceramint.2015.08.140>
- [4] A. Gupta, K. Mondal, A. Sharma, et al., *RSC Adv.* 5, 45897 (2015);
<https://doi.org/10.1039/C5RA02938D>
- [5] P. Y. Kuang, J. X. Low, B. Cheng, et al., *J Mater. Sci. Technol.* 56, 18 (2020);
<https://doi.org/10.1016/j.jmst.2020.02.037>
- [6] Q. Zhong, Y. Li, G. K. Zhang. *Chem. Eng. J* 409, 128099 (2021);
<https://doi.org/10.1016/j.cej.2020.128099>
- [7] M. T. Liu, J. Y. Li, R.M. Bian, et al., *J Alloy Compd.* 905, 164025 (2022);
<https://doi.org/10.1016/j.jallcom.2022.164025>
- [8] W. L. Yu, J. F. Zhang, T. Y. Peng, et al., *Appl. Catal. B-Environ.* 18, 220 (2016).
- [9] T. G. Xu, L. W. Zhang, H. Y. Cheng, et al., *Appl. Catal. B-Environ.* 10, 382 (2011).
- [10] C. F. Fan, J. Shi, Y. W. Zhang, et al., *Nanoscale* 14, 3441 (2022);
<https://doi.org/10.1039/D1NR06838E>
- [11] Y. Cao, Q. H. Deng, Z. D. Liu, et al., *RSC Adv.* 7, 20494 (2017);
<https://doi.org/10.1039/C7RA00184C>
- [12] R. Z. Ou, Z. X. Zeng, X. T. Ning, et al., *Appl. Surf. Sci.* 577, 151856 (2022);
<https://doi.org/10.1016/j.apsusc.2021.151856>
- [13] B. Zeng, R.. Wang, W. Zeng. *Dig. J Nanomater. Bios.* 16, 989 (2021).
- [14] S. Suwanboon, P. Amornpitoksuk, A. Sukolrat, et al., *Ceram. Int.* 39, 2811 (2013);
<https://doi.org/10.1016/j.ceramint.2012.09.050>
- [15] B. Zeng, Z. G. Li, W. J Zeng. *Dig. J Nanomater. Bios.* 16, 627 (2021).
- [16] P. Pascariu, M. Homocianu, C. Cojocaru, et al., *Appl. Surf. Sci.* 476, 16 (2019);
<https://doi.org/10.1016/j.apsusc.2019.01.077>
- [17] R. Mimouni, B. Askri, T. Larbi, et al., *Inorg. Chem. Commun.* 115, 107889 (2020);
<https://doi.org/10.1016/j.inoche.2020.107889>
- [18] M. Abdullah Iqbal, S. Irfan Ali, Faheem Amin, et al., *ACS Omega*, 4, 8661 (2019);
<https://doi.org/10.1021/acsomega.9b00493>
- [19] P. Y. Lin, J. Shen, X. H. Yu, et al., *Ceram. Int.* 45, 24656 (2019);
<https://doi.org/10.1016/j.ceramint.2019.08.203>
- [20] B. Zeng, W. F. Liu, W. J. Zeng. *J Mater. Sci-Mater. EL.* 30, 6846 (2019);
<https://doi.org/10.1007/s10854-019-00997-8>